Materials Characterization 107 (2015) 239–248

Contents lists available at ScienceDirect

Materials Characterization

journal homepage: www.elsevier.com/locate/matchar

Influences of strain rate on the low cycle fatigue behavior of gravity casting Al alloys

K.L. Fan [a,*], X.S. Liu [a], G.Q. He [a], H. Cheng [b,c], Z. Zhang [a]

[a] School of Materials Science and Engineering, Tongji University, Shanghai 201804, China
[b] School of Mechanical Engineering, Tongji University, Shanghai 201804, China
[c] Engineering Practice Center, Tongji University, Shanghai 200092, China

A R T I C L E I N F O

Article history:
Received 11 May 2015
Received in revised form 22 July 2015
Accepted 23 July 2015
Available online 26 July 2015

Keywords:
Al9Si3Cu alloys
Low cycle fatigue
Strain rate
Cyclic deformation
Fracture characteristics

A B S T R A C T

The strain-controlled low cycle fatigue properties were evaluated on specimens of 333 aluminum alloy at different strain rates. The material exhibited initial cyclic hardening followed by cyclic stabilization at the strain rates of 0.15 min^{-1}, 0.20 min^{-1}, 0.30 min^{-1} and 0.32 min^{-1}, while the material showed continuous cyclic hardening at the strain rate of 0.25 min^{-1}. The observed phenomena in hysteresis loops were in accord with the cyclic hardening and stability characteristics. At the strain rates of 0.15 min^{-1} and 0.32 min^{-1}, the cyclic hardening characteristics observed were mainly due to the existence of dislocation network structures, as well as the accumulation of dislocations around some obstacles. The cyclic stabilization observed in both samples was correlated closely with the cross-slip during cycling at the strain rates of 0.15 min^{-1} and 0.32 min^{-1}. At the strain rate of 0.25 min^{-1}, the continued cyclic hardening observed in the specimen was bound up with the evolution of dislocation loops. The fracture surface for the alloy exhibited some dimples and tear ridges at the strain rates of 0.15 min^{-1} and 0.25 min^{-1}, whereas some fatigue striations were observed at the strain rate of 0.32 min^{-1}. The damage process of the 333 aluminum alloy composed of several mixed events: α-Fe/silicon particle cracking, short crack initiation and propagation, and local linkage of short cracks.

© 2015 Elsevier Inc. All rights reserved.

1. Introduction

Cast Al–Si–Cu alloys have widespread applications for making structural components in automobile industry due to their low density, excellent castability, low shrink rate, and relatively high specific strength [1]. Aluminum alloy cylinder heads, as a part of combustion chamber, are frequently subjected to repeated strains, which will lead to plasticity over a period of time. A key issue regarding automotive cylinder heads, therefore, is the strain controlled low cycle fatigue (LCF) performance of the used material. A few experimental investigations and theoretical analyses have been conducted to promote the understanding of the strain controlled LCF mechanisms of Al–Si–Cu alloys, and some significant achievements have been made [2–8]. Some work has been completed on the effect of alloying elements on the cyclic deformation of Al–Si–Cu alloys during LCF. By introducing Zr/V into an Al–Si–Cu alloy, the fatigue life of the material was observed to be somewhat longer than that of only the Zr-modified alloy [2]. Similarly, Shaha and co-workers [3] recently clarified that the intermetallic precipitates containing Zr, Ti and V could improve the fatigue life of the Al–7Si–1Cu–0.5Mg alloy in the T6 condition. They also found that the Zr–Ti–V-containing particles of the examined material characterized by fatigue striations at the low total strain amplitude of 0.002, whereas these particles were featured by multiple cracking along with some micro-cliffs at the high total strain amplitude of 0.006. Other studies have shown that the LCF behaviors of Al–Si–Cu alloys correlated closely with total strain amplitude [4], as well as temperature [5–8]. For instance, early work by the authors has demonstrated that the total strain amplitude could play a crucial role in the LCF of Al9Si3Cu alloys, which in turn affected the fracture modes and crack paths [4]. According to Liu et al. [6], the LCF life of the die casting Al–12Si–CuNiMg alloy increased with increasing temperature (from 473 K to 673 K) under the same total strain amplitude. Recent work by the authors [8] on the cyclic deformation response of Al9Si3Cu alloys produced by gravity casting, however, has demonstrated that the fatigue life of the alloy at 523 K was shorter than that at 423 K at any given total strain amplitude. This was mainly bound up with plasticity, the existence of PFZs together with $AlMg_4Zn_{11}$ precipitates, secondary cracks and Al_xO_y particles.

Generally, the strain-controlled fatigue deformation of a metal is known to be sensitive to the variation of strain rate. Several work on the LCF behavior of metals, such as steels [9,10] and stainless steels [11], has been done in trying to understand the interaction between the fatigue loading and strain rates. To the author's best knowledge, only one group studied the cyclic deformation behavior in aluminum alloys (Al–Si alloys) with various strain rates, where the LCF lifetime at

* Corresponding author at: School of Materials Science and Engineering, Tongji University, No. 4800 Caoan Road, Jiading District, Shanghai 201804, China.
E-mail address: 12klfan@tongji.edu.cn (K.L. Fan).

http://dx.doi.org/10.1016/j.matchar.2015.07.024
1044-5803/© 2015 Elsevier Inc. All rights reserved.

523 K increased with the increase of strain rate, due to higher plastic strain at lower strain rate [12]. Although there are limited reports on the LCF behaviors of Al–Si–Cu alloys, there is no detailed report regarding the effect of different strain rate on the LCF of Al–Si–Cu alloys. In the present study, the strain-controlled LCF behavior was evaluated on samples of GC Al9Si3Cu alloys at different strain rates, which were machined from the automobile engine cylinder heads. The combined fatigue damage mechanism associated with various strain rates was also characterized in this work.

2. Material and experiments

The material utilized in this study was a 333 aluminum alloy with base composition of Si ~ 9.15%, Cu ~ 3.23%, Fe ~ 0.37%, Zn ~ 0.36%, Mg ~ 0.30%, Ni ~ 0.26%, Mn ~ 0.16%, and Sr ~ 0.038%. Samples used for fatigue tests were machined from the spark plug boss of commercial automobile engine cylinder heads, and then were heat-treated to the T6 condition, solution treated at 500 °C for 8 h in an air circulated furnace, followed by artificial aging at 150 °C for 4 h. Dog-bone round samples for fatigue tests were machined with a gauge length of 30 mm. Samples for strain controlled LCF tests were mechanically polished by emery papers in order to minimize surface roughness effects on tests. Fatigue tests were performed in a MTS 809 servo-hydraulic test system (MTS, USA) with an extensometer directly attached to the samples. The tests were conducted with strain rates lying between 0.15 min^{-1} and 0.32 min^{-1}. For investigating the strain rate dependency of the fatigue response of the 333 aluminum alloy, a constant total strain amplitude of 0.003 was utilized. A symmetrical triangular waveform was used under fully-reversed strain-controlled conditions ($R_\varepsilon = -1$). The experiments would be stopped when the stresses dropped about 10%. Table 1 shows the relationship between fatigue life and strain rate in specimens (S1–S10) during tests. Noted that the fatigue life decreased with the increasing strain rate from 0.15 min^{-1} to 0.25 min^{-1}, and then it would increase as the strain rate increased further. Fractography and surface relief observations were performed by scanning electron microscopy (SEM) coupled with energy dispersive X-ray (EDX) facility. Transmission electron microscopy (TEM) was conducted at an acceleration voltage of 200 kV, equipped with a conventional double tilting stage. The gauge sections of the specimens were mechanically thinned for the extraction of TEM foils. The longitudinal portion of the gauge section was first reduced to approximately 500 μm using a slow speed saw. The discs thus obtained were mechanically thinned down to approximately 30 μm using carborundum papers. Large electron-transparent areas were obtained in these foils by conventional twin jet polishing utilizing a solution of 5% $KClO_4$ and 95% CH_3CH_2OH at a temperature of −25 °C.

3. Results and analysis

3.1. Cyclic stress response behavior

Fig. 1 shows the evolution of cyclic stress amplitude at the strain amplitude of 0.003 during LCF tests for different strain rates. For the strain rates studied, the alloy exhibited initial hardening followed by a stability stage (namely, the cyclic stress amplitude remained essentially constant), except at the strain rate of 0.25 min^{-1}, where the material showed a pronounced and continuous cyclic hardening from the first cycle to failure. Moreover, as strain rate increased between 0.15 min^{-1} and 0.25 min^{-1}, the stress amplitude ranges increased. In contrast, the stress amplitude ranges decreased with increasing strain rate from 0.25 min^{-1} to 0.32 min^{-1}.

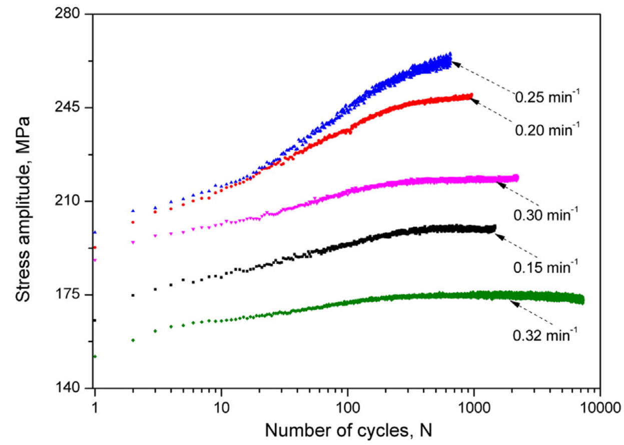

Fig. 1. Stress amplitude vs. the number of cycles for 333 aluminum alloys at different strain rates.

In order to quantify the hardening variation related to various strain rates, the cyclic hardening ratio *H* is computed according to the following equation:

$$H(\%) = \left[(\Delta\sigma/2)_{max} - (\Delta\sigma/2)_1\right]/(\Delta\sigma/2)_1.$$

Here, $(\Delta\sigma/2)_{max}$ denotes the maximum stress amplitude shown during LCF, and $(\Delta\sigma/2)_1$ denotes stress amplitude for the first cycle. The corresponding data from the cyclic hardening ratio evaluations are summarized in Fig. 2. It is evident that cyclic hardening ratio *H* increased with the increasing strain rate in the range of 0.15 min^{-1} to 0.25 min^{-1}. Meantime, cyclic hardening ratio *H* would reach a maximum at the strain rate of 0.25 min^{-1}. Then, instead, *H* would decrease greatly as the strain rate increased further.

3.2. Hysteresis loops

In the sections that follow, three representative samples loaded at strain rates of 0.15 min^{-1} (S1), 0.25 min^{-1} (S5) and 0.32 min^{-1} (S9)

Table 1
Fatigue lives of samples failed under different strain rates.

Sample number	Strain rate (min^{-1})	Fatigue life (cycles)
1	0.15	1471
2	0.15	1387
3	0.20	959
4	0.20	892
5	0.25	652
6	0.25	581
7	0.30	2201
8	0.30	2331
9	0.32	6026
10	0.32	7259

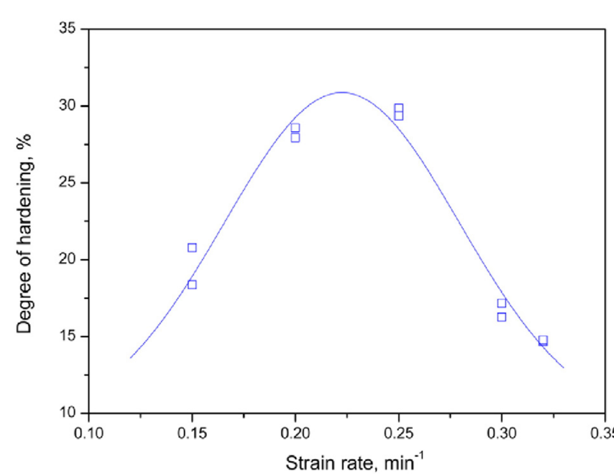

Fig. 2. Degree of hardening *H* for 333 aluminum alloys at different strain rates.

Download English Version:

https://daneshyari.com/en/article/7970184

Download Persian Version:

https://daneshyari.com/article/7970184

Daneshyari.com